Available online at www.sciencedirect.com
ScienceDirect
Journal of Catalysis 247 (2007) 112–118
JOURNAL OF CATALYSIS
www.elsevier.com/locate/jcat

$Cu–Al_2O_3–CuAl_2O_4$ water–gas shift catalyst for hydrogen production in fuel cell applications: Mechanism of deactivation under start–stop operating conditions

Oleg Ilinich *, Wolfgang Ruettinger, Xinsheng Liu, Robert Farrauto

BASF Catalysts LLC, 101 Wood Avenue, Iselin, NJ 08830, USA

Received 11 July 2006; revised 12 January 2007; accepted 23 January 2007

Abstract

This paper analyzes the mechanism of deactivation of a new $Cu–Al_2O_3–CuAl_2O_4$ water–gas shift (WGS) catalyst recently developed for small-scale hydrogen generation applications, such as fuel cell-based residential power generators and hydrogen fueling stations. The catalyst has good potential for use in small-scale fuel processors working under essentially steady-state conditions, such as on-site hydrogen generation systems for hydrogen filling stations. However, transient regimes with frequent starts and stops of the fuel processing system, common for the residential fuel cell applications, can result in aging with a decline in activity of this (and most likely of any) copper-based WGS catalyst. The study described in this paper reveals that the aging resulting in deactivation of $Cu–Al_2O_3–CuAl_2O_4$ under start–stop conditions is due to passivation of the catalytically active surface by the dense shell of hydrogen-bonded hydroxides strongly adsorbed over copper oxide crystallites. This deactivation phenomenon, likely to be typical for all copper-based WGS catalysts operating with frequent starts and stops, is a serious issue that will likely prevent use of such catalysts in residential fuel cell applications. However, the deactivated $Cu–Al_2O_3–CuAl_2O_4$ catalyst can be regenerated by calcining in air, with full recovery of the activity. This regeneration, which is impossible for conventional copper–zinc–alumina catalysts, is a significant practical advantage and also supports the conclusion on the role of surface hydroxides in the deactivation mechanism.

Keywords: Water–gas shift; Copper-based catalyst; Aging; Deactivation; Regeneration

1. Introduction

Industrial technologies of hydrogen and synthesis gas production involve the water–gas shift reaction (WGSR): $CO + H_2O \rightleftarrows CO_2 + H_2$. This moderately exothermic reaction was first used industrially at the beginning of the 20th century as a part of the Haber–Bosch process of ammonia synthesis [1]. The first industrial WGSR catalyst patented by Bosch and Wild was based on iron oxide and operated at high temperatures (up to 600 °C) due to moderate activity [2]. A major step forward in the development of WGSR technology is associated with the invention of copper-based catalysts [3]. Since the 1960s, copper-based catalysts have been widely used in this process for low-temperature operations (ca. 200–250 °C), where thermodynamic equilibrium favors higher CO conversions [4,5].

Conventional copper-based catalysts were designed to operate under steady-state conditions in large-scale industrial plants. They are sensitive to steam condensation and require very careful and lengthy startup and shutdown procedures due to the highly exothermic nature of the catalyst reduction and reoxidation [4,6].

Today, hydrogen-producing technologies are becoming increasingly downscaled and decentralized. This trend is driven by the emerging markets based on relatively small-scale hydrogen production technologies for fuel cell power systems, hydrogen filling stations, and on-site hydrogen generation for various technical needs [6,7]. These new technologies are imposing additional requirements on the properties of WGS catalysts, which must fulfill more stringent safety requirements because they often will be operated unattended and will experience very

* Corresponding author. Fax: +1 732 205 5300.
E-mail address: oleg.ilinich@basf.com (O. Ilinich).

0021-9517/$ – see front matter
doi:10.1016/j.jcat.2007.01.014

different duty cycles than in conventional industrial processes. In particular, the operational model for residential fuel cell power systems currently under development in Japan presumes daily start and stop (DSS) of the system. The DSS mode implies cyclic operation comprising the following elements: (1) rapid heatup of the reactor and start of the reformate flow; (2) several hours of WGS operation, possibly with varying loads; and (3) reformate flow shutoff and reactor cooldown, possibly with exposure to condensing steam. An immediate consequence of these new requirements is a need for a more robust and safe catalyst that can be operated without special precautions typical of conventional copper-based WGS catalysts.

The newly developed Cu–Al_2O_3–$CuAl_2O_4$ WGS catalyst was initially designed for hydrogen-generating fuel processors integrated into fuel cell applications for residential power systems, where the catalysts are subjected to frequent startups and shutdowns. We found that startup/shutdown conditions are the key to the performance of Cu–Al_2O_3–$CuAl_2O_4$ catalyst. In particular, startups and shutdowns with steam condensing on the catalyst stimulate catalyst aging with an activity decline. The deactivated catalyst however can be fully regenerated by calcining in air.

The present paper describes a study of the mechanism of Cu–Al_2O_3–$CuAl_2O_4$ catalyst aging during startups and shutdowns in steam-reach environments, as well as of its regeneration, which has important practical and mechanistic implications.

2. Experimental

2.1. Cu–Al_2O_3–$CuAl_2O_4$ catalyst preparation

The Cu–Al_2O_3–$CuAl_2O_4$ WGSR catalyst was produced as described in detail previously [8], following these steps: (1) mixing pseudoboehmite powder, wood flour, and copper nitrate solution; (2) extruding the mix; (3) drying the extrudates; and (4) calcining in air at 700–800 °C. The resulting catalyst is an oxide compound containing 12 wt% Cu relative to the total weight of the sample and having the monomodal pore structure with average pore diameter ca. 10 nm and BET surface area ca. 100 m^2/g.

2.2. Catalyst activity characterization

Activity tests were performed in a computer-controlled laboratory flow reactor, which enabled continuous operation with programmed profiles of temperature, flow rates, and concentrations of the reactants. The reactor comprised a 2.5-cm-i.d. quartz tube with a fritted quartz disc supporting the catalyst samples. The catalysts were crushed and sieved before the activity tests, with fractions of 355–710 μm used for the measurements. Activity test results obtained with the catalyst particles of the above dimensions were free from pore diffusion limitations. In the activity tests, the catalyst temperature typically was monitored with two thermocouples touching the top of the sample bed (inlet temperature) and the fritted quartz disc supporting the samples (outlet temperature).

All activity tests were conducted under WGS process conditions typical of real-world hydrogen-producing fuel processors, which use authothermal reforming (ATR) as the first stage of hydrocarbon fuel conversion. For the activity tests described in the present communication, the simulated reformate (ATR product gas) of the following composition was used: 5.9% CO, 7.4% CO_2, 31.8% H_2, 28.9% N_2, and 26% H_2O. The catalyst activity was characterized by monitoring the CO concentration at the reactor outlet with an online infrared gas analyzer ZRH (Fuji Electric, Japan).

The samples of Cu–Al_2O_3–$CuAl_2O_4$ catalyst exposed to the reaction conditions and then submitted for characterization were cooled to the room temperature under nitrogen flow before being removed from the reactor, to minimize the effect of air exposure.

2.3. Instrumental techniques of catalyst characterization

The Cu–Al_2O_3–$CuAl_2O_4$ catalyst was characterized by DRIFTS, Raman and CO chemisorption, XRD, and XPS. The DRIFTS spectra were collected on a Bio-Rad FTS-7 spectrometer with a SpectraTec diffuse reflectance attachment. The catalyst samples were treated at 300 °C under flow of either ultra-high purity Ar or of the mixture 30% H_2 + 70% Ar for 1 h and cooled to room temperature before introduction of CO.

The Raman spectra were collected on a Renishaw RM1000 micro-Raman spectrometer with a CCD detector and a 785-nm laser. CO chemisorption was performed on the FTIR instrument in the flow of 1% CO in ultra-high purity argon. XRD data were collected with a Philips vertical goniometer in Cu$K\alpha$ radiation with generator settings of 45 kV and 40 mA. XPS analysis of the catalyst was performed on VG220iXL instrument equipped with monochromatic source Al$K\alpha$ at 10^{-9} Torr residual pressure and pass energy 40 eV.

3. Results and discussion

3.1. Start–stop conditions and the catalyst aging

In developing applications such as fuel cell power generators, the WGSR catalysts are subjected to operational cycles with frequent starts and stops of the reactor. Our catalyst aging tests were designed to mimic performance in those applications. The tests were performed by cycling the reactor inlet temperature between 220 and 70 °C while changing the feed gas composition, as shown in Fig. 1. The catalytic performance was monitored by continuously measuring the outlet CO concentration at 220 °C (gray segment in Fig. 1) with a reformate feed consisting of 5.9% CO, 7.4% CO_2, 31.8% H_2, 28.9% N_2, and 26% H_2O, at GHSV = 2500 h^{-1}. At temperatures below 220 °C (white segment in Fig. 1) the reactor feed in different runs was either reformate, or steam purge (i.e., 45% H_2O + 55% N_2), or CO_2 purge (i.e., 70% CO_2 + 30% N_2). These atmospheres were selected to enable discernment of the catalyst deactivation mode. Note that at 70 °C, water condensed on the catalyst with both reformate and steam purges. The aging test protocols are summarized in Table 1.

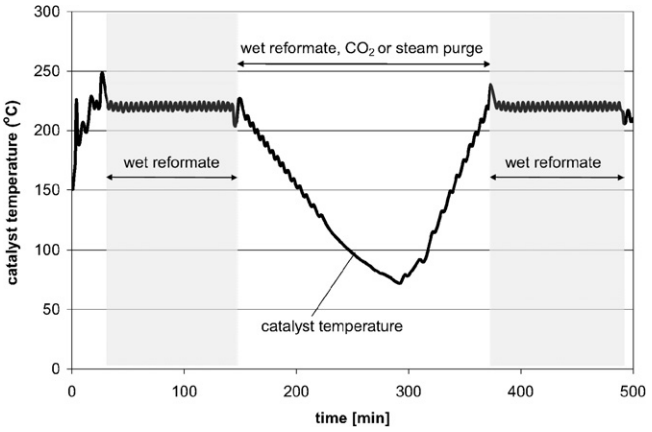

Fig. 1. Catalyst temperature and gas compositions vs time on stream in the simulated start–stop aging tests.

Table 1
Aging test protocols

Test No.	Test conditions
1	Sample pre-reduced by heating up to 220 °C in dry reformate[a]. Wet reformate[b] further used throughout the program
2	Sample pre-reduced by heating up to 220 °C in dry reformate. Wet reformate further used throughout the program at 220 °C, and 45% H_2O + 55% N_2 mixture below 220 °C
3	Sample pre-reduced by heating up to 220 °C in 70% CO_2 + 30% H_2. Wet reformate further used throughout the program at 220 °C, and 70% CO_2 + 30% N_2 mixture below 220 °C

[a] Dry reformate: 8% CO + 10% CO_2 + 43% H_2 + 39% N_2.
[b] Wet reformate: 5.9% CO + 7.4% CO_2 + 31.8% H_2 + 28.9% N_2 + 26% H_2O.

The results of performing the aging cycles are shown in Fig. 2. In this figure, the data points on each curve correspond to the outlet CO concentrations registered at the reaction temperature of 220 °C after the simulated start–stop cycles. Note that a fresh sample of the same batch was used for each aging test. As can be seen, the simulated starts and stops in flowing reformate (curve 1) resulted in a slow aging of the catalyst, steam purge during simulated startups and shutdowns caused faster aging (curve 2), and the dry CO_2 purge (curve 3) produced no catalyst aging. Thus, the loss of activity observed in the reformate start–stop aging test apparently is due to exposure of the catalyst to steam at low temperatures, not to CO_2 as was reported for copper–ceria catalysts [9].

3.2. Regeneration

The Cu–Al_2O_3–$CuAl_2O_4$ catalyst deactivated due to aging can be regenerated by heating in air. Under properly chosen regeneration conditions (i.e., temperature and duration), virtually complete recovery of the initial activity can be achieved.

For the study of regeneration conditions, the sample of Cu–Al_2O_3–$CuAl_2O_4$ catalyst was aged in the above-described start–stop aging test under conditions specified in Fig. 2, curve 2, with a gradual decline in activity observed during 3 weeks of time on stream. After that, regeneration of the aged sample by calcining in air was explored. The activities of fresh,

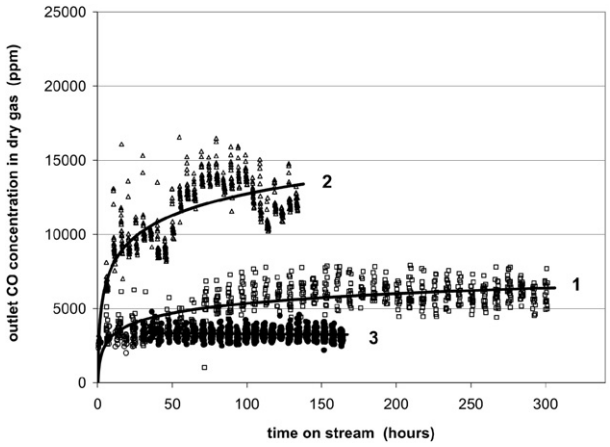

Fig. 2. CO outlet concentration vs time on stream in the aging tests with various start–stop procedures. Test conditions (see Fig. 1): (a) feed gas at 220 °C in all tests: wet reformate; (b) feed gas below 220 °C: curve 1—wet reformate; curve 2—45% H_2O + 55% N_2; curve 3—70% CO_2 + 30% N_2. Catalyst reduction conditions: see Table 2.

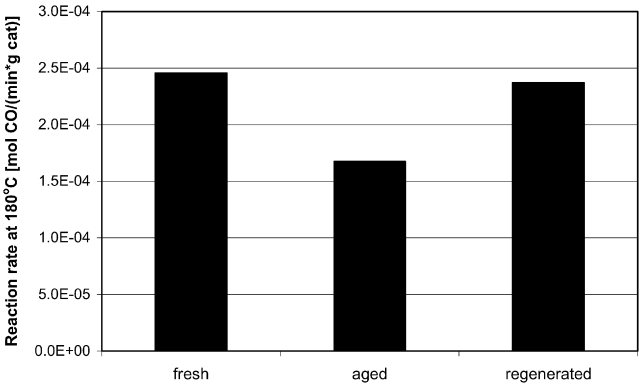

Fig. 3. Reaction rates at 180 °C for the fresh, aged, and regenerated samples of the Cu–Al_2O_3–$CuAl_2O_4$ catalyst. The aging test conditions: 6 h steady-state WGS reaction at 220 °C in feed gas with 5.9% CO, 7.4% CO_2, 31.8% H_2, 28.9% N_2, and 26% H_2O at GHSV = 10,000 h^{-1}, followed by cooling to 65 °C and heating up to 220 °C in the mixture of 45% steam + 55% N_2. The aged sample regeneration conditions: calcinations in air at 750 °C for 30 min.

aged and regenerated samples were compared by running the test described in Section 2.2. The activity test results are summarized in Fig. 3. As can be seen, calcining of the aged and partially deactivated sample in air at 750 °C for 30 min resulted in virtually complete recovery of the activity up to the level registered for the fresh sample. It is important to note that such regeneration, simple and efficient as it is, cannot be performed for a commercial Cu–Zn–Al_2O_3 catalyst due to its sintering at temperatures above ca. 250 °C [4].

The mechanisms of aging and regeneration of the Cu–Al_2O_3–$CuAl_2O_4$ catalyst were investigated using XRD, XPS, and IR techniques.

3.3. Phase composition of the catalyst

The XRD patterns of the as-prepared (fresh) and aged Cu–Al_2O_3–$CuAl_2O_4$ catalyst are shown in Fig. 4. The fresh sample (pattern A) shows diffraction lines that can be assigned to CuO (JCPDS file No. 41-0254), γ-Al_2O_3 (JCPDS file No. 10-

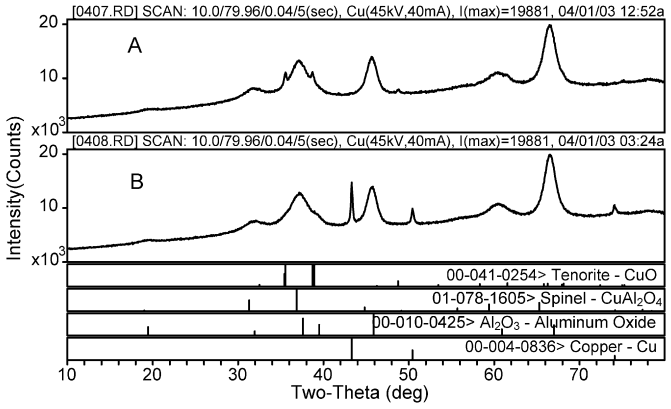

Fig. 4. XRD patterns of the Cu–Al_2O_3–$CuAl_2O_4$ catalyst. Pattern A: as-prepared (fresh) catalyst; Pattern B: the catalyst aged in the start–stop test. The aging test conditions: 6 h steady-state WGS reaction at 220 °C in feed gas with 5.9% CO, 7.4% CO_2, 31.8% H_2, 28.9% N_2 and 26% H_2O at GHSV = 10,000 h^{-1}, followed by cooling to 65 °C and heating up to 220 °C in the mixture of 45% steam + 55% N_2.

0425) and copper–alumina spinel $CuAl_2O_4$ (JCPDS file No. 33-0448), with Al_2O_3 and the spinel possibly forming a solid solution. Note that very similar patterns were recently reported for the copper–alumina catalysts prepared by impregnation of γ-Al_2O_3 with copper nitrate, followed by calcinations in air at 800 °C [10]. Formation of the spinel in the Cu–Al_2O_3–$CuAl_2O_4$ catalyst is a result of the preparation method [8], which includes calcination in air at 700–800 °C.

After aging in WGS reaction, the phase composition of the catalyst changes so that two of the three initially present phases (γ-Al_2O_3 and $CuAl_2O_4$) remain intact, while CuO reduces to metallic Cu (Fig. 4, pattern B). Note that the latter was detected as such even though for the XRD analysis, the sample was exposed to air after being cooled in nitrogen flow as described in Section 2.2. XRD analyses of samples treated under different WGS conditions have shown that the phase composition of the Cu–Al_2O_3–$CuAl_2O_4$ catalyst after reaction was essentially the same independent of the particular process conditions, including steady-state or start–stop operations with different purge conditions. XRD patterns of the aged Cu–Al_2O_3–$CuAl_2O_4$ catalyst, which was further regenerated by calcining in air at 750 °C, were essentially identical to those of the fresh as-prepared catalyst.

3.4. Cu/CuO crystallite size

Crystallite size values calculated from the XRD data for the identified Cu-bearing phases in each sample are summarized in Table 2. Although the values of the crystallite sizes should be treated with some caution, because the aged sample was exposed to air after aging as described in Section 2.2, the sizes of copper–bearing crystallites appear similar for the fresh and aged samples. No evidence of copper sintering with the Cu–Al_2O_3–$CuAl_2O_4$ catalyst aging was found by TEM analysis of the same samples.[1]

[1] G.R. Munzing, unpublished results.

Table 2
Crystallite size for Cu-bearing phases in Cu–Al_2O_3–$CuAl_2O_4$ catalyst

Sample condition	CuO(202) [nm]	Cu(200) [nm]
Fresh	34.1	–
Aged under conditions of test No. 2, Table 1	–	37.9

Table 3
XPS data summary for fresh and aged Cu–Al_2O_3–$CuAl_2O_4$ catalyst (the sample was aged under conditions of test No. 2, Table 1)

Element and valence	Surface composition	
	Fresh sample	Aged sample
Al (Al_2O_3)	33.4	35.3
Cu^0 and/or Cu^+	0	0.45
Cu^{2+}	4.3	3.7
Atomic ratio		
Cu/Al	0.13	0.12

3.5. Surface composition of Cu–Al_2O_3–$CuAl_2O_4$ catalyst by XPS

XPS analysis was performed for fresh and aged samples of the Cu–Al_2O_3–$CuAl_2O_4$ catalyst. The experimental data are summarized in Table 3. As can be seen, exposure of the catalyst to WGS environment results in the appearance of the low-valence copper species such as Cu^0 and Cu^+, whereas the fresh material contains Cu only as Cu^{2+}. Because the aged sample was exposed to air before the XPS examination, the detected amounts of copper species in this sample do not characterize the surface composition of the catalyst under WGS conditions. Instead, these data illustrate partial reoxidation of the catalyst when the sample conditioned in WGS environment is exposed to air at room temperature. This low-temperature reoxidation apparently affects only a thin surface layer, because XRD analysis did not detect copper oxides in the aged sample.

Surface composition of the aged Cu–Al_2O_3–$CuAl_2O_4$ catalyst regenerated by calcining in air at 750 °C was essentially the same as that of the fresh as-prepared catalyst. Thus, the results of XRD and XPS analyses indicate that a common factor in catalyst aging—sintering of the active phase—is not responsible for the deactivation of the Cu–Al_2O_3–$CuAl_2O_4$ catalyst under WGS conditions.

The mechanism of the catalyst aging and regeneration was further investigated using IR spectroscopy techniques.

3.6. IR study of the mechanism of Cu–Al_2O_3–$CuAl_2O_4$ catalyst aging

As discussed in Section 3.1, contacting the Cu–Al_2O_3–$CuAl_2O_4$ catalyst at relatively low temperatures with steam-containing process gas has a profound negative effect on the activity and operational lifetime of the catalyst. It follows from the results of XRD and XPS studies given above that sintering is not the cause of the Cu–Al_2O_3–$CuAl_2O_4$ catalyst aging. Therefore, two other factors need to be examined to find out the possible cause of the catalyst aging associated with steam: (i) surface reconstruction of the active phase and (ii) blocking of the active surface by species generated from the process gas.

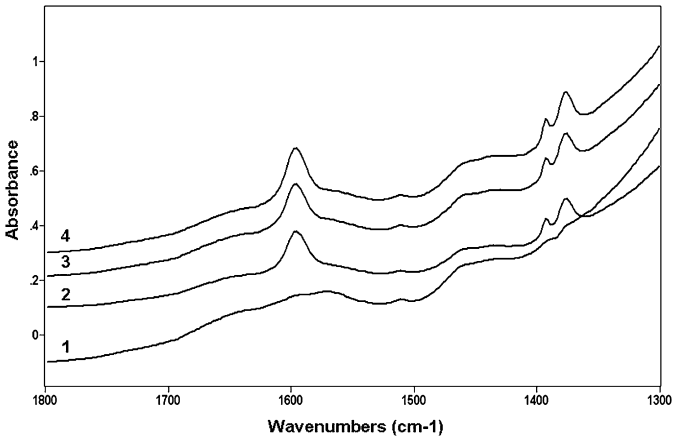

Fig. 5. DRIFT spectra of the $Cu–Al_2O_3–CuAl_2O_4$ catalyst samples of different histories, reduced at 300 °C for 1 h under flow of 30% H_2 + 70% Ar mixture: (1) fresh sample; (2) sample aged by temperature cycling with 70% CO_2 + 30% N_2 purge; (3) sample aged by temperature cycling with continuously flowing reformate; (4) sample aged by temperature cycling with 45% steam + 55% N_2 purge.

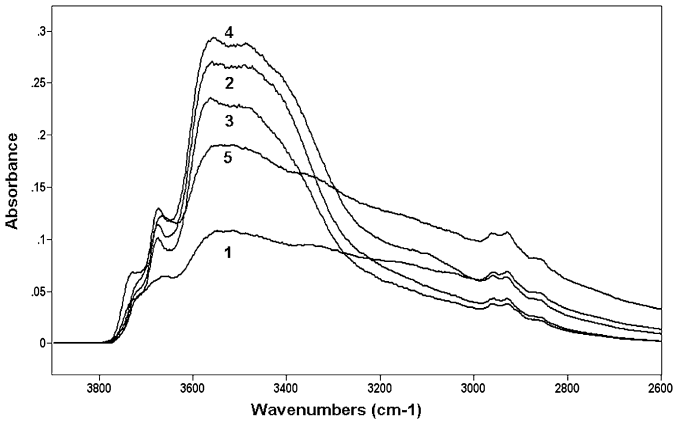

Fig. 6. DRIFT spectra of $Cu–Al_2O_3–CuAl_2O_4$: (1) fresh sample; (2) sample aged by temperature cycling with 70% CO_2 + 30% N_2 purge; (3) sample aged by temperature cycling with continuously flowing reformate; (4) sample aged by temperature cycling with 45% steam + 55% N_2 purge; (5) sample regenerated by heating in air at 700 °C for 1 h after aging as in (4).

It is known from the literature that reconstruction of the active surface may occur on some Cu-based catalysts, depending on support materials used. However, surface reconstruction was not observed for copper catalysts supported on alumina, even though it might occur on zinc oxide-supported copper and copper–zinc–alumina catalysts [11,12]. Blocking of the active surface by carbonate species was found on platinum–ceria [13], palladium–ceria [14], and gold–ceria [15,16] WGS catalysts. For the copper-containing WGS catalysts, carbonate species strongly bound to the catalyst surface were recently suggested to be the cause of deactivation of copper–ceria catalysts [9]. A possibility of $Cu–Al_2O_3–CuAl_2O_4$ catalyst deactivation via the surface blocking mechanism was investigated in the present study. The samples of $Cu–Al_2O_3–CuAl_2O_4$ catalyst of the following histories were analyzed: (1) fresh, (2) aged by temperature cycling with a 70% CO_2 + 30% N_2 purge during simulated shutdowns/startups, (3) aged by temperature cycling with continuously flowing reformate, (4) aged by temperature cycling with 45% steam + 55% N_2 purge during simulated shutdowns/startups, and (5) regenerated by heating in air at 750 °C for 30 min after aging, as in (4). The aging procedures and aging behaviors of these samples are described in detail in Section 3.1.

3.6.1. Surface carbonates

DRIFT spectra in the spectral region 1800–1300 cm^{-1} of the catalyst samples with different histories are shown in Fig. 5. Note that all samples except the fresh sample had been previously exposed to WGS conditions for the activity testing. The spectra were collected after the samples were heated under 30% H_2 + 70% Ar mixture flow at 300 °C for 1 h. This treatment was chosen to mimic the reducing conditions typical of the WGS reaction. The data represented in Fig. 5 show that the fresh sample (spectrum 1) contains a trace amount of monodentate carbonate species (weak band at 1510 cm^{-1}) [17]. This band does not change in intensity with aging, indicating that the species are not disturbed under the aging conditions. On aging the catalyst in the simulated start–stop test with 70% CO_2 + 30% N_2 purge, the spectrum of the sample now includes bands at 1596, 1392, and 1377 cm^{-1} (spectrum 2) that are associated with bidentate carbonates [17]. The bidentate carbonates do not affect the activity of the catalyst, as was demonstrated in the activity tests conducted for this series of samples; that is, the sample aged in the simulated start–stop tests with 70% CO_2 + 30% N_2 purge showed no aging. This implies that the carbonates are most likely associated with the alumina. Similar deposition is also observed for the samples aged in the simulated start–stop tests with continuously flowing reformate and with inert purges of high steam concentration (spectra 3 and 4).

Correlating the carbonate IR band intensity with the catalyst performance shows no relationship between the amount (i.e., peak intensities) of the bidentate surface carbonates and the activities of the samples in the simulated start–stop tests with the corresponding purges. Our tests showed that the activities of the above samples after aging fell into the following order: sample (2) treated with dry CO_2 > sample (3) treated with reformate > sample (4) treated with steam. Thus, we conclude that catalyst deactivation observed in the start–stop tests with steam contacting the catalyst at relatively low temperatures is not associated with the deposition of surface carbonates, in contrast to what was found for CeO_2-supported catalysts [9,13–16].

3.6.2. Surface hydroxyls

Fig. 6 shows DRIFTS spectra in the 3900–2800 cm^{-1} spectral region of $Cu–Al_2O_3–CuAl_2O_4$ catalyst samples with different histories. This spectral region is characteristic of the surface OH groups [18–20]. The bands at around 3720 and 3670 cm^{-1} are due to OH groups associated with alumina, whereas the broad bands at around 3500 cm^{-1} extending to 2800 cm^{-1} are due to hydrogen-bonded OH groups. The broad spectral feature at 3400–2800 cm^{-1} of the fresh sample (spectrum 1) implies the presence of hydrogen-bonded OH groups belonging to both Cu^{2+} and Cu^{+} hydroxides (overlapping with those bands on alumina). The presence of Cu^{2+} and Cu^{+} hydroxides

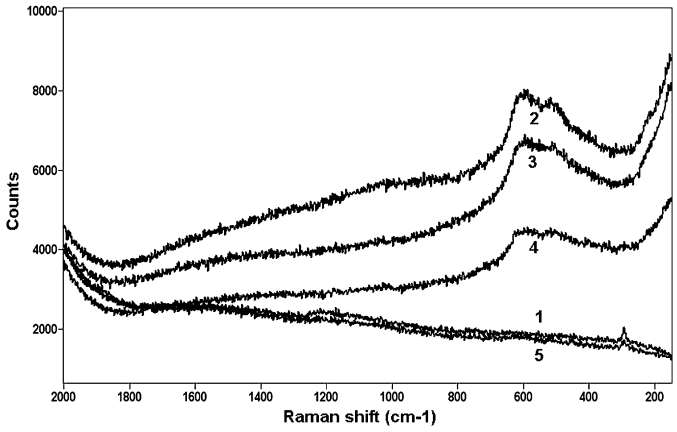

Fig. 7. Raman spectra of $Cu–Al_2O_3–CuAl_2O_4$ catalyst samples. The spectra are labeled as in Fig. 6.

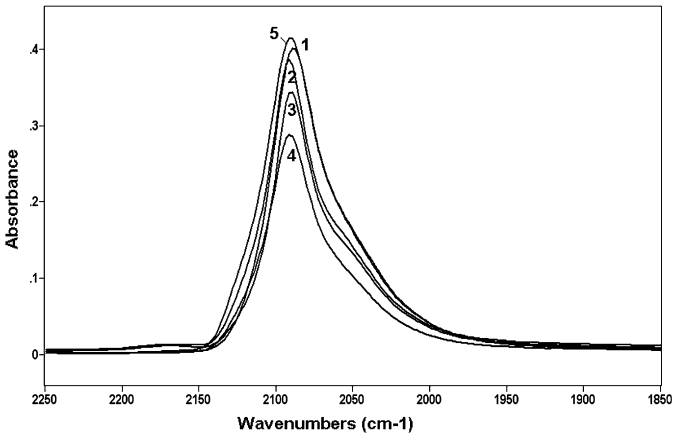

Fig. 8. DRIFT spectra of CO chemisorbed on the samples of different histories, reduced at 300 °C for 1 h under flow of 30% H_2 + 70% Ar mixture before introduction of CO: (1) fresh sample; (2) sample aged by temperature cycling with 70% CO_2 + 30% N_2 purge; (3) sample aged by temperature cycling with continuously flowing reformate; (4) sample aged by temperature cycling with 45% steam + 55% N_2 purge; (5) sample regenerated by heating in air at 700 °C for 1 h after aging as in (4).

was confirmed by Raman spectroscopy (Fig. 7), where the band at 292 cm^{-1} is due to CuO and the bands at 600 and 503 cm^{-1} are associated with $Cu(OH)_2$ and/or CuOH [21,22].

On aging the sample in the simulated start–stop test with the 70% CO_2 + 30% N_2 dry purge, the following IR spectral changes are observed: The band at around 3000 cm^{-1} decreases in intensity, whereas the band at around 3500 cm^{-1} increases in intensity (spectrum 2 in Fig. 6). These changes are accompanied by reduction of CuO [and/or $Cu(OH)_2$] to Cu_2O and/or CuOH, as demonstrated by the disappearance of the 292-cm^{-1} band characteristic of CuO (the phase observed by XRD analysis) and/or $Cu(OH)_2$ that could also be present as an amorphous surface compound and the appearance of the 600- and 503-cm^{-1} bands characteristic of Cu_2O and/or CuOH in the corresponding Raman spectrum (spectrum 2 in Fig. 7) [23]. Aging in the simulated start–stop tests with steam-containing purges further enhances the 3500 cm^{-1} bands (spectra 3 and 4 in Fig. 6), indicating that more OH groups are generated on the surface of copper oxide crystallites. Regeneration by calcining in air of the sample aged due to steam exposure strongly decreases the intensity of the 3500-cm^{-1} OH bands (spectrum 5 in Fig. 6) and restores the CuO band (spectrum 5 in Fig. 7).

Comparing these spectral changes with the catalyst performance data described above (Section 3.2.1) reveals a correlation of the OH group band intensity with the degree of catalyst deactivation; the higher the intensity of the broad 3500 cm^{-1} band, the stronger the catalyst deactivation. This result indicates that the formation of hydrogen-bonded OH groups on the surface of copper oxide crystallites (Cu^+ and/or Cu^{2+}) is the main cause of a catalyst deactivation in the start–stop cycles with steam contacting the catalyst at low temperatures. This further means that along with acting as a WGS reactant, steam also may have an undesirable side effect by acting as an aging agent under "wet" process startup/shutdown conditions when water may condense on the catalyst.

Fig. 8 represents DRIFTS spectra of CO chemisorbed on the samples aged under different conditions as well as on the fresh and regenerated samples. All samples were reduced at 300 °C in the 30% H_2 + 70% Ar mixture before chemisorption. As one can see, CO chemisorption is the greatest on the fresh sample (spectrum 1). Aging under different conditions causes a decrease in CO uptake, reflecting diminution of the Cu metal surface available for CO adsorption due to oxidation of copper. Note that the oxidized copper sites in the aged samples cannot be completely reduced under the chosen reduction conditions. The regenerated sample (spectrum 5) shows a complete recovery of the Cu surface, with CO adsorption increasing to the level observed in the fresh sample. The changes in CO uptake correlate well with the catalyst performance in the WGS reaction.

From the foregoing results, it can be concluded that the carbonate species present on the surface of the $Cu–Al_2O_3$ catalyst are not the cause of catalyst aging in simulated start–stop aging cycles. The catalyst deactivation occurring in those cycles is due to the surface hydroxylation of copper oxide crystallites. The hydroxides, strongly adsorbed over copper oxide sites, block the catalytic surface, rendering it inactive for WGS reactions. The surface hydroxides cannot be removed by reduction of the catalyst with hydrogen at 300 °C; however, air calcination of the aged catalyst destroys the hydroxide shell and regenerates the catalytic sites. Note that a similar regeneration of a commercial copper–zinc–alumina WGS catalyst is not possible, due to its massive sintering at temperatures above about 250 °C.

4. Conclusions

This work elucidates mechanistic aspects of aging of a new $Cu–Al_2O_3–CuAl_2O_4$ WGS catalyst operating under conditions typical of fuel reformers integrated to residential fuel cell systems, which involve frequent startups and shutdowns. It is concluded that catalyst aging under these conditions is due to formation of hydrogen-bonded surface hydroxyls strongly adsorbed on the oxidized surface of copper-bearing crystallites and blocking the catalytically active sites. As the steam-containing process gas (reformate) contacts the catalyst in its oxidized state at relatively low temperatures (typically on startup of a fuel processor), the copper oxide crystallites are

covered with the dense shell of hydrogen-bonded surface hydroxides. The hydroxides are stable under the WGS conditions and substantially reduce the amount of copper available for the catalytic cycle. This is a dominant aging factor in the start–stop operating regime typical of small-scale residential fuel cell power generators.

The ability of a deactivated catalyst to regenerate by calcining in air is an important practical aspect. Moreover, it confirms the crucial role of the surface hydroxides in the deactivation mechanism.

Essential features of the above-described mechanism are likely to be applicable to other copper-based WGS catalysts. Therefore, due to their inherent sensitivity to frequent startups and shutdowns typical of stand-alone residential power systems, copper-based catalysts are an unlikely choice for fuel processors integrated into fuel cell generators for residential applications. However, the new regenerable copper-based WGS catalysts with improved operational and environmental safety features have a good potential for acceptance in other developing technologies that do not require frequent starts and stops, such as distributed hydrogen generation units.

Acknowledgments

The authors are grateful to their colleagues Nancy Brungard, Thomas Gegan, and George Munzing for conducting the XPS, XRD, and TEM analyses of Cu–Al_2O_3–$CuAl_2O_4$ catalyst.

References

[1] K. Holdermann, Im Banne der Chemie: Carl Bosch Leben und Werk, Econ-Verlag, Düsseldorf, 1953.
[2] C. Bosch, W. Wild, Canadian patent 153 379 (1914), to BASF.
[3] A.T. Larson, U.S. patent 1 797 426 (1931), to DuPont Ammonia Corporation.
[4] L. Lloyd, D.E. Ridler, M.V. Twigg, in: M.V. Twigg (Ed.), Catalyst Handbook, second ed., Wolfe Publishing, Frome, 1989, p. 283.
[5] D.S. Newsome, Catal. Rev. Sci. Eng. 21 (1980) 275.
[6] J.R. Ladebeck, J.P. Wagner, in: W. Vielstich, A. Lamm, H.A. Gasteiger (Eds.), Handbook of Fuel Cells—Fundamentals, Technology and Applications, vol. 3, Wiley, New York, 2003, p. 190.
[7] R. Farrauto, S. Hwang, L. Shore, W. Ruettinger, J. Lampert, T. Giroux, Y. Liu, O. Ilinich, in: K.D. Kreuer, D.R. Clarke, M. Rühle, J.C. Bravman (Eds.), Annual Review of Materials Research, vol. 33, Annual Reviews, Palo Alto, 2003, p. 1.
[8] O.M. Ilinich, W.F. Ruettinger, R.T. Mentz, R.J. Farrauto, U.S. patent 6 903 050 (2005), to Engelhard Corporation.
[9] X. Wang, J.A. Rodrigues, J.C. Hanson, D. Gamarra, A. Martinez-Arias, M. Franandez-Garcia, J. Phys. Chem., ACS ASAP 2005.
[10] H. Yahiro, K. Nakaya, T. Yamamoto, K. Saiki, H. Yamaura, Catal. Commun. 7 (2006) 228.
[11] N.-Y. Topsøe, H.J. Topsøe, Mol. Catal. A Chem. 1999 (1999) 95.
[12] B.H. Sakakini, J. Tabatabaei, M.J. Watson, K.C. Waugh, J. Mol. Catal. A 162 (2000) 297.
[13] X. Liu, W.F. Ruettinger, X. Xu, R.J. Farrauto, Appl. Catal. B 56 (2005) 69.
[14] S. Hilaire, X. Wang, T. Luo, R.J. Gorte, J. Wagner, Appl. Catal. A 258 (2004) 271.
[15] C.H. Kim, L.T. Thompson, J. Catal. 230 (2005) 66.
[16] Q. Fu, W. Deng, H. Saltsburg, M. Flytzani-Stephanopoulos, Appl. Catal. B 56 (2005) 57.
[17] A. Davydov, Molecular Spectroscopy of Oxide Catalyst Surfaces, Wiley, New York, 2003, p. 134.
[18] X. Liu, R.E. Truitt, J. Am. Chem. Soc. 119 (1997) 9856.
[19] A.A. Tsyganenko, P.P. Mardilovich, J. Chem. Soc. Faraday Trans. 92 (1996) 4843.
[20] C. Morterra, G. Magnacca, Catal. Today 27 (1996) 497.
[21] J.F. Xu, W. Ji, Z.X. Shen, W.S. Li, S.H. Tang, X.R. Ye, D.Z. Jia, X.Q. Xin, J. Raman Spectrosc. 30 (1999) 413.
[22] P.Q. Larson, A. Andersson, J. Catal. 179 (1998) 72.
[23] J. Tong, Y. Matsumura, Catal. Today 111 (2006) 147.